Published in final edited form as:
J Neurochem. 2009 July ; 110(1): 157–169. doi:10.1111/j.1471-4159.2009.06110.x.

Normal protein composition of synapses in Ts65Dn mice, a mouse model of Down syndrome

Fabian Fernandez[1,4], **Jonathan C. Trinidad**[2,4], **Martina Blank**[1], **Dong-Dong Feng**[3], **Alma L. Burlingame**[2,*], and **Craig C. Garner**[1,*]

[1]Department of Psychiatry and Behavioral Sciences, Nancy Pritzker Laboratory, Stanford University, Palo Alto, CA 94304

[2]Mass Spectrometry Facility, Department of Pharmaceutical Chemistry, University of California, San Francisco, CA 94143

[3]Department of Neurology, Stanford University, Palo Alto, CA 94304

Abstract

Down syndrome is the most prevalent form of intellectual disability caused by the triplication of ~ 230 genes on chromosome 21. Recent data in Ts65Dn mice, the foremost mouse model of Down syndrome, strongly suggest that cognitive impairment in individuals with Down syndrome is a consequence of reduced synaptic plasticity due to chronic over-inhibition. It remains unclear however whether changes in plasticity are tied to global molecular changes at synapses, or are due to regional changes in the functional properties of synaptic circuits. One interesting framework for evaluating the activity state of the Down syndrome brain comes from *in vitro* studies showing that chronic pharmacological silencing of neuronal excitability orchestrates stereotyped changes in the protein composition of synaptic junctions. In the present study, we use proteomic strategies to evaluate whether synapses from the Ts65Dn cerebrum carry signatures characteristic of inactive cortical neurons. Our data reveal that synaptic junctions do not exhibit overt alterations in protein composition. Only modest changes in the levels of synaptic proteins and in their phosphorylation are observed. This suggests that subtle changes in the functional properties of specific synaptic circuits rather than large-scale homeostatic shifts in the expression of synaptic molecules contribute to cognitive impairment in people with Down syndrome.

Keywords

Down syndrome; Ts65Dn; plasticity; synapse; PSD; mass spectrometry

Down syndrome (DS), triplication of human chromosome 21 (HSA21), is a condition that results in moderate to profound intellectual disability (Brugge *et al.* 1994; Lejeune *et al.* 1959). Over the past century, there have been intense efforts to better understand what attributes of the DS brain are coincident with cognitive impairment. In turn, these efforts have highlighted general decreases in brain weight (a function of cerebral and cerebellar atrophy, shortened occipital lobes, and narrowing of the superior temporal gyri), and particular deficits in pyramidal cell dendritic arborization and dendritic spine architecture (Davidoff 1928; Schmidt-Sidor *et al.* 1990). For example, dendritic branching and spine

[*]Correspondence Craig C. Garner, Ph.D., Department of Psychiatry and Behavioral Sciences, Nancy Pritzker Laboratory, Stanford University, 1201 Welch Rd, Palo Alto, CA 94304. cgarner@stanford.edu. [*]Alma L. Burlingame, Ph.D., Mass Spectrometry Facility, Department of Pharmaceutical Chemistry, University of California, San Francisco, 600 16th Street, San Francisco, CA 94143. alb@cgl.ucsf.edu.
[4]These authors contributed equally to the work.

counts in the hippocampus (Ferrer and Gullota 1990; Suetsugu and Mehraein 1980), in layers III and V of visual cortex (Takashima *et al.* 1981; Becker *et al.* 1986), and in layers of the motor cortex (Marin-Padilla 1972; Marin-Padilla 1976) are dramatically reduced in people with DS. Moreover, the remaining spines in the visual and motor cortices adopt irregular morphologies: some spines appear long and tortuous, while others develop enlarged heads (all features of synaptic contacts with reduced plastic or learning potential; Marin-Padilla 1976; Takashima *et al.* 1981). Intriguingly, the emergence of these cytological phenotypes tends to parallel the beginning of IQ decline in DS-affected children within the first few years of life (Nadel 2003), further suggesting that the loss of cognitive performance is directly coupled to a loss of plasticity at synapses during early stages of development.

Investigation of nervous system abnormalities and cognitive dysfunction in DS has been greatly facilitated by the development of the mouse model Ts65Dn (Davisson *et al.* 1990; Reeves *et al.* 1995) which is segmentally trisomic for approximately 110 of the 230 genes found on HSA21 (Akeson *et al.* 2001). Ts65Dn mice faithfully recapitulate some of the most fundamental features of DS, showing craniofacial (Richtsmeier *et al.* 2000; Richtsmeier *et al.* 2002) and cerebellar abnormalities (Baxter *et al.* 2000; Olson *et al.* 2004), and nearly comprehensive deficits in declarative memory (Bimonte-Nelson *et al.* 2003; Demas *et al.* 1996; Demas *et al.* 1998; Escorihuela *et al.* 1995; Escorihuela *et al.* 1998; Holtzman *et al.* 1996; Hunter *et al.* 2003; Hyde and Crnic 2001; Wenger *et al.* 2004). Moreover, the cytological changes in spine morphology observed in persons with DS are also present in several parts of the Ts65Dn brain, including the hippocampus, motor and somatosensory cortices (Belichenko *et al.* 2004). Such similarities between Ts65Dn and individuals with DS suggest that phenotypes characterized in the mice might translate well to the condition in people.

In the past decade a series of studies looking at synaptic connections within the Ts65Dn brain have suggested that reduced learning in Ts65Dn mice is due to altered function of excitatory synapses in the hippocampal formation. In the absence of GABA-A receptor blocking reagents, excitatory synapses in CA1 and dentate gyrus are unable to undergo long-term potentiation (LTP) - the electrophysiological correlate of learning and memory (Belichenko *et al.*, 2004; Costa and Grybko 2005; Fernandez *et al.* 2007; Kleschevnikov *et al.* 2004; Kurt *et al.*, 2000; Siarey *et al.* 1997; Siarey *et al.* 1999). This deficit in synaptic plasticity might result from either molecular changes in synaptic constitution or changes in neuronal circuits which are linked by extensive synaptic connections.

Ultrastructurally, excitatory synapses are comprised of a presynaptic terminal and an adjacent postsynaptic structure that is usually situated on the heads of large mushroom-shaped dendritic spines. Both compartments contain complex protein matrices. The presynaptic active zone is a specialized region of plasma membrane that is equipped with release machineries which organize vesicle-mediated exocytosis of neurotransmitter into the synaptic cleft. The postsynaptic density (PSD) is a molecular scaffold that confines postsynaptic receptors and links postsynaptic receptor activation to myriad downstream signaling moieties (for review, see Sheng and Hoogenraad 2007; Waites *et al.* 2005; Ziv and Garner 2004).

Despite the tightly organized structure of pre- and post-synaptic sites, synapses have been shown to be highly plastic with regard to their size and protein composition. For example, changes in postsynaptic receptor number in response to synaptic activity are traditionally thought to lead to long-term modifications in synaptic strength, such as LTP and long-term depression (LTD) (Malinow and Malenka 2002). More recently, another form of plasticity has been described wherein chronic (but not acute) shifts in the activity levels of neural

circuits lead to altered synapse morphology and/or composition (Turrigiano *et al.* 1998). This form of plasticity is now commonly referred to as ”homeostatic plasticity” (Turrigiano and Nelson 2000). A seminal study relating to homeostatic plasticity by Ehlers (2003) suggested that chronic pharmacological silencing of cultured neurons orchestrates stereotyped changes in the proteomic makeup of the PSD, as neurons attempt to compensate for reduced synaptic transmission by increasing the responsiveness of the postsynapse.

In the present study, we address whether chronic changes in excitability in Ts65Dn mice (Fernandez *et al.* 2007; Fernandez and Garner 2007) can be linked to global changes in the protein composition of synapses *in vivo*. To that end, we prepared synaptosomes or PSD's from the Ts65Dn cerebrum and evaluated synaptic protein profiles via two quantitative methods: Odyssey-based fluorescence western blotting or quantitative mass spectrometry using the iTRAQ (isobaric tag for relative and absolute quantitation) reagent. While the former allowed us to carefully evaluate a number of key synaptic proteins known to respond to chronic activity states in synaptosomal preparations, the latter represented a comprehensive screen of hundreds of proteins associated with the PSD.

Materials and Methods

Synaptosomal and PSD Fractionation

Segmental trisomy 16 (Ts65Dn) mice were obtained by mating female carriers of the 17^{16} chromosome (B6EiC3H – a/ATs65Dn) with (C57BL/6JEi × C3H/HeJ)F1 (JAX # JR1875) males. Ts65Dn mice were thus maintained on the B6/C3H background. Wildtype (WT) and Ts65Dn littermates with at least one functional *Rd* allele (3 months old; Jax West Laboratories, Davis, CA) were euthanized via CO_2 inhalation (n = 4–6 experimental pairs, per cohort). The cerebri *sans* cerebella were immediately removed, flash-frozen in liquid nitrogen, and homogenized in Tris Buffer-A [40mM Tris, pH 7.5] containing 0.3M sucrose, 1.6 mg/ml protease inhibitor cocktail (Roche Applied Science), and phosphatase inhibitors: 1mM NaF, 1mM Na-molybdate, 1mM Na-tartrate, 1mM Na_3VO_4, 100nM Fenvalerate, and 250nM Okadaic acid (Sigma); [ratio of tissue to buffer, 1:10]. Subsequently, homogenized samples were cleared by centrifugation at 1000 *g* for 10 min (4°C). The membranous fraction was separated from the cytosolic fraction at 17 000 *g* for 20 min, and submitted to density centrifugation (120 min, 85 000 *g*) using a gradient consisting of 0.8 M, 1.0 M, and 1.2 M sucrose in Tris Buffer-A. The resulting synaptosomal fraction was collected at the 1.0–1.2 M interface, diluted with Tris Buffer-A, pelleted (20 min, 78 500 *g*), and stored at −80°C.

For PSD preparations, synaptosomes were further homogenized in 10mM Bicine Buffer (pH 7.5) containing 5% *N*-octyl-beta-*D*-glucopyranoside (NOG, Calbiochem, San Diego, CA, USA), phosphatase inhibitors and protease inhibitors, and applied onto a second discontinuous gradient (1.0 M, 1.4 M, 2.2 M sucrose in 10 mM bicine pH 7.5, containing 1% NOG and phosphatase inhibitors; 120 min, 85 000 *g*) as diagramed in Supplementary Figure 1. The PSD fraction was collected at the 1.4–2.2 M interface, diluted in 10mM bicine pH 7.5 and pelleted by centrifugation (20 min, 78 500 *g*) before storing at −80°C.

Quantitative Fluorescence Western Blotting

Protein concentration was determined (in triplicate) using the Bradford assay. Samples (6 μg) were denatured in loading buffer containing sodium dodecyl sulfate (SDS; 8%) and dithiothreitol (1mM), separated by polyacrylamide gel electrophoresis (7.5%; BioRad), and transferred to a nitrocellulose membrane (Hybond ECL, Amersham, Piscataway, NJ). Equal loading and transfer of material in each lane was verified by Ponceau staining; note that total protein stains might be a more accurate loading control than immunodetection of high-

abundance single proteins (Aldridge *et al.* 2008). The membranes were then washed in TBS, blocked in TBS containing 5% milk (Carnation), and probed with the following antibodies: mouse anti-Rim1/2 (1:1000; BD Transduction Laboratories), mouse anti-Munc13 (1:250; BD Transduction Laboratories), mouse anti-clathrin heavy chain (1:1000; a gift from R. Jahn), mouse anti-synaptojanin (1:500; BD Transduction Laboratories), rabbit anti-Erc/CAST2 (1:1000; a gift from Y. Takai), rabbit anti-CASK (1:1000; Zymed), mouse anti-synapsin1 (1:2000; Synaptic Systems), mouse anti-Munc18 (1:1000; BD Transduction Laboratories), mouse anti-synaptotagmin (1:500; a gift from R. Jahn), rabbit anti-VGluT1 (1:1000; a gift from R. Reimer), rabbit anti-VGAT (1:2500; a gift from R. Reimer), mouse anti-CtBP1 (1:2500; BD Transduction Laboratories), rabbit anti-GAP43 (1:1000; Chemicon), rabbit anti-synaptophysin (1:4000; Santa Cruz), mouse anti-SNAP25 (1:500; a gift from R. Jahn), mouse anti-GKAP (pan; 1:500; a gift from S. Kindler), rabbit anti-NR2A (1:1000; Novus), rabbit anti-NR2B (1:1000; Molecular Probes); rabbit anti-neurabin1/spinophilin (1:500; a gift from S. Shenolikar), mouse anti-NR1 (1:1000; BD Transduction Laboratories), rabbit anti-SAP102 (1:4000; a gift from J. Hell), rabbit anti-PSD95 (1:500; a gift from J. Hell), mouse anti-alpha-tubulin (1:1000; Sigma), mouse anti-tyrosinated-tubulin (1:1000; Sigma), rabbit anti-$GABA_A\alpha 1$ (1:1000; Upstate Biotechnology), mouse anti-CaMKIIα (1:1000; Zymed), and rabbit anti-phospho-ERK p42/p44 (1:500; Cell Signaling Technology). Detection of bound primary antibodies was performed with fluorescently-conjugated goat anti-rabbit (Alexa Fluor 680, 1:30 000, Molecular Probes, Invitrogen, Carlsbad, CA) or goat anti-mouse (Rockland IRDye 800, 1:5000, Rockland Immunochemicals, Inc., Gilbertsville, PA) secondary antibodies. Immunofluorescence was detected and analyzed using the Odyssey imaging system (LI-COR Biosciences, Lincoln, NE). Please note that samples from 4 independent WT and Ts65Dn experimental pairs were analyzed. Synaptosomes from one of these WT-Ts65Dn pairs were run together on one gel in duplicate or triplicate. Each synaptic protein in our survey was probed at least twice – meaning that data were always collected from at least 2 of the 4 experimental pairs.

Mass Spectrometry Analysis: Sample Preparation

A more detailed description of the mass spectrometry analysis can be found in Trinidad *et al* (2008). In brief, for digestion of PSD samples, 500 μg aliquots of material were processed in parallel. Each PSD sample was resuspended in 25 mM ammonium bicarbonate, containing 6 M guanidine hydrochloride. The mixture was incubated for one hour at 57°C with 2 mM Tris (2-carboxyethyl) phosphine hydrochloride to reduce cysteine side chains. These side chains were then alkylated with 4.2 mM iodoacetamide in the dark for 45 min at 21°C. The resulting mixture was diluted six fold with 25 mM ammonium bicarbonate, and 5% (w/w) modified trypsin (Promega, Madison, WI, USA) was added. Thereafter, the pH was adjusted to 8.0 and the mixture was digested for 12 hours at 37°C. The digests were desalted using a C18 Sep Pak cartridge (Waters, Milford, MA, USA) and lyophilized to dryness using a SpeedVac concentrator (Thermo Electron, San Jose, CA, USA).

Mass Spectrometry Analysis: iTRAQ Labeling and Strong Cation Exchange Chromatography

500 μg of tryptic peptides from each sample were labeled with iTRAQ reagent following the manufacturer's suggestion with slight modifications (Trinidad *et al.* 2008). Strong cation exchange (SCX) chromatography was used to initially fractionate the labeled peptide mixture. This was performed using an ÄKTA Purifier (GE Healthcare, Piscataway, NJ, USA) equipped with a Tricorn 5/200 column (GE Healthcare, Piscataway, NJ, USA) packed in-house with 5 μm 300 Å polysulfoethyl A resin (Western Analytical, Lake Elsinore, CA, USA). The 2.0-mg combined PSD sample was loaded onto the column in 30% acetonitrile, 5 mM KH_2PO_4, pH 2.7 (Buffer A). Buffer B consisted of Buffer A with 350 mM KCl. The gradient went from 1% B to 29% B over 19 ml, from 29% B to 75% B over 14 ml, and from

75% B to 100% B over 2.5 ml. 5% of each fraction was reserved for analysis using an ESI-Qq-TOF tandem MS, while the remaining 95% was subjected to immobilized metal affinity chromatography as previously described (Trinidad *et al.* 2006). Peptide fractions were analyzed on a QSTAR Pulsar mass spectrometer (Applied Biosystems, Foster City, CA, USA). For each MS spectrum, the two most intense multiple charged peaks were selected for generation of subsequent collision-induced dissociation MS.

Mass Spectrometry Analysis: Interpretation of MS/MS Spectra

Data were analyzed using Analyst QS software (version 1.1), and MS/MS centroid peak lists were generated using the Mascot.dll script (version 1.6b18). The MS/MS spectra were searched against the entire Uniprot *Mus musculus* database (downloaded April 19, 2007, with a total of 64,717 entries) using the following parameters: 1.) initial peptide tolerances in MS and MS/MS modes were 200 ppm and 0.2 daltons, respectively; 2.) trypsin was designated as the enzyme and up to two missed cleavages were allowed; 3.) carbamidomethylation and iTRAQ labeling of lysine residues were searched as fixed modifications; 4.) the peptide amino termini were fixed as either iTRAQ modified or protein N-terminal acetylated; 5.) oxidation of methionine was allowed as a variable modification; and 6.) phosphorylation of serine/threonine/tyrosine residues were only allowed for titanium dioxide-enriched fractions. Subsequently, all high scoring peptide matches (expectation value < 0.01) from individual LC-MS/MS runs were used to internally recalibrate MS parent ion m/z values within that run. Recalibrated data files were then searched with a peptide tolerance in MS mode of 50 ppm. The output of both searches was combined into a single output file for identification purposes. Proteins identified with single peptides were accepted with Protein Prospector expectation values ≤ 0.001. Proteins identified by multiple peptides were accepted if one of the peptides had an expectation value ≤ 0.01. False identification rates against a randomized-concatenated database were: protein level = 0.81%, peptide level = 0.08%, phosphopeptide level = 0.43%. Protein accession numbers were mapped onto the corresponding UniGene entries (www.ncbi.nlm.nih.gov/sites/entrez?db=unigene), and proteins were condensed to single proteins for quantification and identification purposes if they matched to the same UniGene entry. Peptides that corresponded to proteins from more than one UniGene entry were not used for quantification. All phosphopeptides were manually inspected to verify that the majority of high abundance peaks were *y* or *b* sequence ions, or *y*-H_20/H_3PO_4 or *b*-H_2O/H_3PO_4 ions when appropriate. Site assignments were done manually with the assistance of an in-house site assignment script. A threshold of 25 counts was set for peaks in the iTRAQ diagnostic ion region. Please note that only peptides with at least one peak above threshold were used for quantification.

Results

Quantification of Protein Levels in Synaptosome Preparations

The quantitative reliability of the Odyssey imaging system was validated using synaptosomal fractions prepared from WT mouse brain. First, antibodies directed against each of the synaptic proteins in our survey (at concentrations specified in **Materials and Methods**) were calibrated to determine the dynamic range of signal detection. Loading 1, 3, 6, 9 and 11 μg of synaptosomal material, we found that the infrared signal generated by each antibody was generally linear between 3- and 9-μg (see Fig. 1A for representative signal plots). In subsequent studies, we evaluated the reproducibility of our Western blot procedure. Here, we loaded synaptosomal material (in 6- and 9-μg triplicates) across 3 separate blots, and probed simultaneously for the membrane associated-guanylate kinase homology (MAGUK) protein SAP102 and the α_1 subunit of the $GABA_A$ receptor. As shown in Fig. 1B, there was a close agreement between SAP102 and α_1 signals within each blot and between blots, suggesting that precise amounts of protein could be identified and compared

from one blot to another using the Odyssey system. Thus, given a defined amount of synaptosome (3–9 μg) we could detect all the presynaptic and postsynaptic proteins in our survey in a linear manner and do so with significant reproducibility (Fig. 1C).

Next, quantitative differences in the protein composition of WT and Ts65Dn synaptosomes (prepared from 4 independent, experimental pairs of WT-Ts65Dn littermates) were systematically assessed using 6 μg of sample – the center of the linear range. The kinds of alterations that we had expected at Ts65Dn synapses are molecular adaptations that occur in response to homeostatic plasticity (Turrigiano and Nelson 2000). Fundamentally, these molecular responses involve scaling of AMPA and $GABA_A$ receptor numbers. However, work from Ehlers (2003) also suggests that chronic changes in excitability completely refashion protein ensembles within the PSD. Chronic activity blockade with tetrodotoxin in cortical culture induces a coordinated departure from the synapse of particular glutamate receptor subunits such as the NR2A subunit of the NMDA receptor, particular MAGUK adaptors that traffic and stabilize glutamate receptors in the PSD such as PSD-95, and particular kinases involved with activity-dependent signal transduction such as CaMKIIα. Compensatory increases in other protein ensembles are observed as well, with recruitment of SAP102 and the NR2B subunit of the NMDA receptor. Accompanying this differential trafficking and/or retention of PSD constituents is altered NMDA-mediated signaling to downstream effectors. Chronic activity deprivation robustly increases levels of phosphorylated p44/p42 MAPK (ERK 1/2) in response to glycine application, while nearly abolishing phosphorylation of CREB. Reciprocal molecular changes in PSD composition and effector signaling are observed when activity is chronically elevated in culture with bicuculline. The physiological significance of these respective synaptic profiles remains unclear at the present time, but it is likely that coordinated changes in protein complexes differentially influence the sensitivity of the synapse to LTP and LTD-inducing stimuli.

The homeostatic plasticity model notwithstanding, Ts65Dn synapses showed relatively few changes outside of those expected from gene triplication (e.g., synaptojanin). For instance, synaptosomes prepared from WT and Ts65Dn mice exhibited no differences in their content of VGluT or VGAT (presynaptic transporters necessary for the vesicular uptake of glutamate and GABA, respectively), suggesting that the total number of excitatory and inhibitory vesicles was conserved. Moreover, there were no fluctuations in the levels of several other presynaptic proteins, such as synapsin (an actin-binding protein that regulates the size of the readily-releasable and reserve pools of synaptic vesicles; Greengard *et al.* 1993), synaptotagmin (a putative calcium sensor in the presynaptic terminal; Geppert *et al.* 1994), and synaptophysin (a classic vesicle-associated protein; Sudhof 1987). Proteins integral to presynaptic forms of LTP also remained unchanged, namely Rim1/2, Munc-13 and Munc-18 (Fig. 2A, left set of panels; Table 1). On the postsynaptic side, a number of proteins that are upregulated or downregulated in an activity-dependent manner (Ehlers 2003) were maintained in Ts65Dn, including the NMDA receptor subunits NR1, NR2A and NR2B, SAP102, spinophilin, and phospho-ERK p42/p44. Nonetheless, Ts65Dn synapses did demonstrate some homeostatic-like signatures, with very modest reductions in PSD-95, CaMKIIα and $GABA_A$ α_1 (Fig. 2B, right set of panels; Table 1; $*p < 0.05$). Considering that these reductions were subtle (i.e., 15–20%), we would conclude that the greater constitution of the Ts65Dn synapse is fundamentally intact and that activity-dependent changes are either absent or only expressed at a restricted subpopulation of synapses. By the nature of our analysis – using whole cerebri as starting material for subcellular fractionation – we can not preclude the possibility that the small changes we observed or failed to observe were diluted by mixing substrate more affected by trisomy with that which was less affected.

Mass Spectrometry Quantification of Protein Levels in PSD preparations

PSD fractions were isolated from WT and Ts65Dn mouse brains using a two-step sucrose density gradient centrifugation protocol which includes limited solubilization by the non-ionic detergent *N*-octyl-beta-*D*-glucopyranoside – an extraction method that allows for the maintenance of sensitive but otherwise legitimate protein-protein interactions. Western blot analysis was used to confirm that the final PSD fraction did not possess immunoreactivity to the presynaptic marker synaptophysin. While the resulting preparations are highly enriched for postsynaptic proteins, a limited number of presynaptic proteins are reproducibly isolated using this method, possibly due to their tight interactions with trans-synaptic proteins (Trinidad *et al.* 2006; Walikonis *et al.* 2000). Two independent biological replicates were isolated. Each replicate consisted of two samples: pooled brains from 6 WT mice, paired with pooled brains from 6 Ts65Dn littermates. The resulting set of four PSD preparations (WT1; Ts65DN1; WT2; Ts65DN2) were digested with trypsin and chemically labeled with the iTRAQ reagent. This allowed for simultaneous relative quantification of both WT:Ts65Dn PSD preparations. The peptide mixture was fractionated using strong cation exchange chromatography and analyzed by reverse phase liquid chromatography coupled to an ESI-QTOF mass spectrometer – resulting in the identification and quantification of 922 unique proteins on the basis of 1 or more unique peptides (Fig. 3; **Supplementary Table S1**). Noteworthy, our PSD preparation was not completely free of contaminating proteins (whose abundance will likely vary from preparation to preparation). Because these contaminents generally occur at low levels, we focused our subsequent analysis on those proteins identified by three or more unique peptides (a total of 442 proteins; Supplementary Table S1A). For each protein, the WT/Ts65DN ratio was calculated for both independent sets of PSD preparations. The distribution of $\log_{10}$-averaged WT/Ts65DN ratios is shown in Fig. 3A. Positive ratios indicate that a given protein was, on average, more abundant in the WT PSD preparations, while a negative ratio indicated that it was more abundant in the Ts65Dn PSD preparations. Over 95% of the proteins measured had $\log_{10}$-based expression values between −0.108 and 0.108, corresponding to WT/Ts65DN ratios between 0.78 and 1.28. This narrow, symmetrical distribution suggested that there were no wholesale shifts in protein expression between WT and Ts65Dn PSD's. In addition, Figs. 3B and 3C show the distribution of proteins annotated in the Gene Ontology as synaptic (http://go.princeton.edu) along with a subset of synaptic proteins we have previously characterized as being enriched in the hippocampus (Trinidad *et al.* 2008). In both cases, these subsets also displayed a narrow, symmetrical distribution. Surprisingly, these results suggest that the few modest changes observed in the synaptic expression of proteins at the synaptosomal level do not penetrate to the PSD level. This interpretation is bolstered by the fact that trisomy-related proteins which are over-expressed in synaptosomes as expected (e.g., synaptojanin; Table 1) are found at normal levels in the PSD preparations (**Supplementary Table S1**). The reason for this discrepancy is unclear, but might be due to the tight regulation of protein trafficking thought to occur within the PSD lattice. Table 2 lists those proteins exhibiting the largest consistent increase or decrease in WT/Ts65Dn (DS) ratios from both PSD preparations.

We then examined the relative expression of phosphopeptides quantified in our analysis. Fig. 3D summarizes the $\log_{10}$-averaged WT/Ts65DN ratios for 641 phosphorylated peptides (black bars). By and large, values for the $\log_{10}$ WT/Ts65DN phosphopeptide ratios were normally distributed around a median of 0.0. With only two independent sample replicates, it is a bit difficult to make statistically definitive conclusions about differences in the phosphorylation state of WT versus Ts65Dn PSD's. Nevertheless, several phosphopeptides appeared to be particularly and consistently altered in Ts65Dn samples, including those associated with NMDA receptor complexes (Table 3, and Supplementary Tables S2A–2B).

The general distribution of phosphopeptides appears broader than that of the protein-level distribution. Still, the phosphorylation data is based upon single peptide measurements,

whereas each protein value represents the average of however many peptides were identified for that protein. Therefore, from an averaging point of view, it is not surprising *per se* that the protein values have a narrower range. To assess more directly if the distribution of phosphorylation levels was different, we examined the $\log_{10}$-averaged WT/Ts65DN peptide ratios for all non-phosphorylated peptides from proteins that we found to be phosphorylated (Fig. 3D, white bars). As expected, it was broader than the protein ratio histogram in Fig. 3A. The distribution of phosphorylated peptides showed an overall reduction in WT/Ts65DN ratio (i.e., a relative increase in phosphorylation in Ts65Dn synapses relative to WT ones). Here, the median WT/Ts65DN ratio of phosphorylated peptides was 7.3% less than that of the non-phosphorylated peptides (0.944 relative to 1.018; $p < 0.001$, Student's *t*-test) – a significant but subtle shift.

These data, together with our Western blot analysis, suggest that the trisomic condition in Ts65Dn does not lead to substantial changes in protein composition at excitatory synapses and that deficits in cognition are likely to reside in changes in the physiological properties of specific neural circuits.

Discussion

It has recently been proposed by several groups that developmental intellectual disabilities are rooted in alterations at synaptic junctions (Chechlacz and Gleeson 2003; Fernandez and Garner 2007; Zoghbi 2003). In keeping with this suggestion, partial Mmu16 trisomy and reduced excitability are both predicted to alter the normal stochiometry of proteins at Ts65Dn DS excitatory synapses. Here, we report that synaptosomes and PSD's isolated from the cerebri of adult Ts65Dn mice show no overt changes in their protein composition and only modest changes if any in protein expression. However, shifts in the phosphorylation of a number of synaptic proteins were observed. Our data suggest that the trisomic condition primarily serves to change the functional state of synaptic proteins, but does not result in a fundamental reorganization of synapses.

While gross changes in synaptic composition were not observed in this study, we did observe modest changes in a few synaptic proteins present in synaptosomal preparations. Increased levels of synaptojanin, a presynatic protein involved in coordinating a network of accessory factors associated with clathrin-mediated synaptic vesicle recycling (Dresbach *et al.* 2001), are consistent with its gene being present on HSA21 and also triplicated in Ts65Dn mice. The increased levels found in our study (WT/Ts65Dn ratio of 0.57 for synaptojanin in synaptosome preparation; Table 1) are predicted to influence the rate of synaptic vesicle endocytosis and perhaps the expression and/or function of non-triplicated presynaptic proteins. Our quantitative Western analysis also detected modest, but significant decreases (~15–20%) in the levels of four synaptic proteins. These include the presynaptic active zone protein ERC1/CAST2/ELKS, the PSD proteins PSD-95 and CaMKIIα, as well as the α1 subunit of the $GABA_A$ receptor (Table 1). ERC1/CAST2/ELKS is a structural protein of the presynaptic active zone (Deguchi-Tawarada *et al.* 2004). The functional significance of its reduction is unclear, though studies in *C. elegans* and *Drosophila* suggest that orthologues of the active zone protein may contribute to the assembly and stability of synapses (Dai *et al.* 2006; Patel *et al.* 2006; Wagh *et al.* 2006). PSD-95 is a core structural protein of the PSD lattice, and is critical for the tethering of AMPA type glutamate receptors within the PSD (Elias *et al.* 2006), as well as the trans-synaptic cell-adhesion molecule Neuroligin (Sudhof 2008). Decreases in the levels of these proteins would correspond to weaker synapses, which are typically situated on thin spines with a smaller number of AMPA receptors (Elias *et al.* 2008). CaMKIIα is a critical regulatory kinase of the PSD and dendritic spines that directly participates in NMDA receptor dependent synaptic plasticity

such as occurs during the induction of LTP (Malenka and Bear 2004). Loss of CaMKIIα from synaptosomes is likewise consistent with weak un-potentiated synapses.

Unlike synaptosomes, we observed no overt changes in protein expression in PSD preparations from Ts65Dn mice. The few synaptic proteins found to exhibit slight changes (e.g., 20–35% decrease) include Munc13, Fragile X mental retardation protein (FMRP), the β subunit of the voltage-dependent calcium channel (VGCC), and liprinα Similar to ERC1/CAST2/ELKS, Munc13, β of VGCC and Liprinα are involved in aspects of presynaptic function such as synaptic vesicle priming, activity dependent influx of calicum and the structural organization of the active zone, respectively (Schoch and Gundelfinger 2006). FMRP is found both pre- and post-synaptically, and is involved in the translation of dendritically localized mRNAs (Galvez and Greenough 2005; Willemsen *et al.* 2004). Again, though it is diffcult to predict how these subtle changes will alter synaptic function, their lower levels are generally consistent with the notion of weaker synapses formed onto thin spines.

Over-inhibition in Ts65Dn would be expected to chronically hinder excitability in the brain, triggering molecular (i.e., compositional) and structural homeostatic changes in dendritic spines geared towards increasing the sensitivity of the postsynapse to incoming stimuli. Despite these expectations, we found little evidence indicating that the basic constitution of Ts65Dn synapses was significantly different from that of WT. For example, NMDA receptor subunits NR1, NR2A, and NR2B were unaltered in both synaptosomes and PSD fractions. Other proteins regulating receptor function and localization such as scaffolding molecules and kinases were either unchanged (SAP102; pERK1/2) or subtly down regulated (PSD-95; CamKIIα) in synaptosomes. Interestingly, we found no evidence of increased levels of $GABA_A$ receptors at synapses suggesting that over-inhibition is not a consequence of enhanced inhibitory postsynaptic responsiveness. The subtle decrease of $GABA_A$ receptor α1 subunit observed in synaptosomes might indicate a compensatory down-regulation of inhibitory receptors in response to over-inhibition. Since homeostatic changes can occur at the level of synapse composition, synapse number, or even neuron numbers, it is possible that changes in spine morphology or in the number of synapses as seen in Ts65Dn mice and people with DS represent compensatory responses to an altered activity state in the brain.

All in all, the biochemical data presented here are consistent with other reports showing little change in the expression of a host of excitatory and inhibitory synaptic proteins in the Ts65Dn brain (Table 4). Indeed, using Western blot of whole hippocampal extracts from adult mice, investigators have found no major shifts in the expression of presynaptic proteins such as synapsin, postsynaptic receptors such as GluR1, NR1 or $GABA_A$α1, or in the expression of trafficking/scaffolding molecules such as PSD-95, neuroligins 1 and 2, and gephyrin (Pollonini *et al.* 2008;Siddiqui *et al.* 2008;Belichenko *et al.* 2009). Levels of proteins involved in signaling cascades associated with learning and memory, CaMKIIα and ERK1/2, also remain stable in the Ts65Dn condition (Siarey *et al.* 2006;Siddiqui *et al.* 2008). However, this relative stability is belied by significant changes in the phosphorylation state of glutamatergic receptors and their signaling effectors which have a role in communicating synaptic activity from the postsynapse to the nucleus (Siarey *et al.* 2006;Siddiqui *et al.* 2008). These findings nicely complement our phospho-proteomic data (Table 3, and **Supplementary Table S2**) showing that peptides from a variety of synaptic proteins including pre- and post-synaptic scaffold proteins and receptors (e.g., Piccolo, Synapsin, Liprin, Dynamin, PSD-95, NMDA receptors, etc.) are altered. This strongly suggests that shifts in the activity of both phosphatases and kinases within neurons in the trisomic condition are modifying the activity of key synaptic proteins.

One caveat to the current work is that we evaluated synapses as constitutive rather than kinetic organelles. In reality, the processes that underlie synaptic plasticity and adult learning and memory are predicated on the dynamic movement of molecules in and out of the synapse in response to activity, such as CaMKIIα recruitment to spines after NMDA receptor activation (Shen *et al.* 2000) or, conversely, synapsin dispersal (Chi *et al.* 2001). They are also dependent on the proper turnover of protein pools with defined exchange rates, allowing synapses to have a stable background with which to sense patterned activity. Accordingly, though the constitutive support structure appears normal at Ts65Dn synapses, it remains an open question as to whether synaptic proteins in Ts65Dn mice demonstrate the same kinetic parameters as WT ones. As such, live imaging of Ts65Dn synapses will be an important area of future investigation.

In summary, the current study argues that cognitive impairment in people with DS cannot be easily reduced to compositional changes at excitatory synapses. Instead, it might emerge from higher order deficits in neural circuits including their glial partners – astrocytes – which have been demonstrated to participate in synaptic transmission to balance excitation and inhibition, and which have a known role in triggering oxidative stress in the DS brain (Busciglio *et al.* 2002; Fellin *et al.* 2006). In this regard, it is important to note that synapses in the hippocampus can undergo changes in synaptic strength in the presence of $GABA_A$ receptor antagonists (Costa and Grybko 2005; Fernandez *et al.* 2007; Kleschevnikov *et al.* 2004) arguing that basic features of synaptic plasticity at excitatory hippocampal synapses are intact.

Interestingly, Hanson *et al.* (2007) have recently shown that the functional nature of synaptic connectivity in the CA3 auto-associative network is modified in organotypic slices prepared from the Ts65Dn hippocampus. Herein, CA3-CA3 connections were more abundant in Ts65Dn mice, as was the number of active versus silent synapses. Considering that these modifications could be relevant to degraded pattern separation and decreased memory capacity in individuals with DS, these data raise the possibility that analogous circuit changes in various other parts of the brain might underlie the spectrum of DS-associated cognitive problems. That said, further systems-based experiments in Ts65Dn await to be conducted.

Supplementary Material

Refer to Web version on PubMed Central for supplementary material.

Acknowledgments

We express our gratitude to the National Science Foundation (F.F.), the National Institute of Health (F.F.), Fondation Jérôme Lejeune (F.F.), the Down syndrome Research and Treatment Foundation (M.B., C.C.G.), the Hillblom Foundation (M.B., C.C.G.), as well as the Stanford Center for Research and Treatment of Down Syndrome (M.B., C.C.G.) and the NIH NCRR Biomedical Research Technology Program Grants RR01614 and RR14606 (A.L.B.) for their support. We would also like to thank the Nelson laboratory at Stanford University for use of their equipment.

Abbreviations

DS	Down syndrome
HSA21	human chromosome 21
PSD	postsynaptic density
MAGUK	membrane associated-guanylate kinase homology

iTRAQ	isobaric tags for relative and absolute quantification
LTP	long-term potentiation
LTD	long-term depression

References

Akeson EC, Lambert JP, Narayanswami S, Gardiner K, Bechtel LJ, Davisson MT. Ts65Dn - localization of the translocation breakpoint and trisomic gene content in a mouse model for Down syndrome. Cytogenet. Cell. Genet. 2001; 93:270–276. [PubMed: 11528125]

Aldridge GM, Podrebarac DM, Greenough WT, Weiler IJ. The use of total protein stains as loading controls: an alternative to high-abundance single-protein controls in semi-quantitative immunoblotting. J. Neurosci. Methods. 2008; 172:250–254. [PubMed: 18571732]

Baxter LL, Moran TH, Richtmeier JT, Troncoso J, Reeves RH. Discovery and genetic localization of Down syndrome cerebellar phenotypes using the Ts65Dn mouse. Hum. Mol. Genet. 2000; 9:195–202. [PubMed: 10607830]

Becker LE, Armstrong DL, Chan F. Dendritic atrophy in children with Down's syndrome. Ann. Neurol. 1986; 20:520–526. [PubMed: 2947535]

Belichenko PV, Masliah E, Kleschevnikov AM, Villar AJ, Epstein CJ, Salehi A, Mobley WC. Synaptic structural abnormalities in the Ts65Dn mouse model of Down syndrome. J. Comp. Neurol. 2004; 480:281–298. [PubMed: 15515178]

Belichenko PV, Kleschevnikov AM, Masliah E, Wu C, Takimoto-Kimura R, Salehi A, Mobley WC. Excitatory-inhibitory relationship in the fascia dentata in the Ts65Dn mouse model of down syndrome. J. Comp. Neurol. 2009; 512:453–466. [PubMed: 19034952]

Bimonte-Nelson HA, Hunter CL, Nelson ME, Granholm A-CE. Frontal cortex BDNF levels correlate with working memory in an animal model of Down syndrome. Behav. Brain Res. 2003; 139:47–57. [PubMed: 12642175]

Brugge KL, Nichols SL, Salmon DP, Hill LR, Delis DC, Aaron L, Trauner DA. Cognitive impairment in adults with Down's syndrome: similarities to early cognitive changes in Alzheimer's disease. Neurology. 1994; 44:232–238. [PubMed: 8309564]

Busciglio J, Pelsman A, Wong C, Pigino G, Yuan M, Mori H, Yankner BA. Altered metabolism of the amyloid beta precursor protein is associated with mitochondrial dysfunction in Down's syndrome. Neuron. 2002; 33:677–688. [PubMed: 11879646]

Chechlacz M, Gleeson JG. Is mental retardation a defect of synapse structure and function? Pediatr. Neurol. 2003; 29:11–17. [PubMed: 13679116]

Chi P, Greengard P, Ryan TA. Synapsin dispersion and reclustering during synaptic activity. Nat. Neurosci. 2001; 4:1187–1193. [PubMed: 11685225]

Costa ACS, Grybko MJ. Deficits in hippocampal CA1 LTP induced by TBS but not HFS in the Ts65Dn mouse: A model of Down syndrome. Neurosci. Lett. 2005; 382:317–322. [PubMed: 15925111]

Dai Y, Taru H, Deken SL, Grill B, Ackley B, Nonet ML, Jin Y. SYD-2 Liprin-alpha organizes presynaptic active zone formation through ELKS. Nat Neurosci. 2006; 9:1479–1487. [PubMed: 17115037]

Davidoff LM. The brain in Mongolian Idiocy. Arch. Neurol. Psychiatr. 1928; 20:1229–1257.

Davisson MT, Schmidt C, Akeson EC. Segmental trisomy of murine chromosome 16: A new model system for studying Down syndrome. Prog. Clin. Biol. Res. 1990; 360:263–280. [PubMed: 2147289]

Deguchi-Tawarada M, Inoue E, Takao-Rikitsu E, Inoue M, Ohtsuka T, Takai Y. CAST2: identification and characterization of a protein structurally related to the presynaptic cytomatrix protein CAST 2. Genes Cells. 2004; 9:15–23. [PubMed: 14723704]

Demas GE, Nelson RJ, Krueger BK, Yarowsky PJ. Spatial memory deficits in segmental trisomic Ts65Dn mice. Behav. Brain Res. 1996; 82:85–92. [PubMed: 9021073]

Demas GE, Nelson RJ, Krueger BK, Yarowsky PJ. Impaired spatial working and reference memory in segmental Trisomy (Ts65Dn) mice. Behav. Brain Res. 1998; 90:199–201. [PubMed: 9521551]

Dresbach T, Qualmann B, Kessels MM, Garner CC, Gundelfinger ED. The presynaptic cytomatrix of brain synapses. Cell. Mol. Life Sci. 2001; 58:94–116. [PubMed: 11229820]

Ehlers MD. Activity level controls postsynaptic composition and signaling via the ubiquitin-proteasome system. Nat. Neurosci. 2003; 6:231–242. [PubMed: 12577062]

Elias GM, Funke L, Stein V, Grant SG, Bredt DS, Nicoll RA. Synapse-specific and developmentally regulated targeting of AMPA receptors by a family of MAGUK scaffolding proteins. Neuron. 2006; 52:307–320. [PubMed: 17046693]

Elias GM, Nicoll RA. Synaptic trafficking of glutamate receptors by MAGUK scaffolding proteins. Trends Cell Biol. 2007; 17:343–352. [PubMed: 17644382]

Escorihuela RM, Fernandez-Teruel A, Vallina IF, Baamonde C, Lumbreras MA, Dierssen M, Tobena A, Florez J. A behavioral assessment of Ts65Dn mice: A putative Down syndrome model. Neurosci. Lett. 1995; 199:142–146.

Escorihuela RM, Vallina IF, Martınez-Cue C, Baamonde C, Dierssen M, Tobena A, Florez J, Fernandez-Teruel A. Impaired short- and long-term memory in Ts65Dn mice, a model for Down syndrome. Neurosci. Lett. 1998; 247:171–174. [PubMed: 9655620]

Fellin T, Pascual O, Haydon PG. Astrocytes coordinate synaptic networks: balanced excitation and inhibition. Physiology. 2006; 21:208–215. [PubMed: 16714479]

Fernandez F, Garner CC. Over-inhibition: A model for developmental intellectual disability. TINS. 2007; 30:497–503. [PubMed: 17825437]

Fernandez F, Morishita W, Zuniga E, Nguyen J, Blank M, Malenka RC, Garner CC. Pharmacotherapy for cognitive impairment in a mouse model of Down syndrome. Nat. Neurosci. 2007; 10:411–413. [PubMed: 17322876]

Ferrer I, Gullota F. Down's syndrome and Alzheimer's disease: dendritic spine counts in the hippocampus. Acta Neuropathol. 1990; 79:680–685. [PubMed: 2141748]

Galvez R, Greenough WT. Sequence of abnormal dendritic spine development in primary somatosensory cortex of a mouse model of the fragile X mental retardation syndrome. Am J Med Genet A. 2005; 135:155–160. [PubMed: 15880753]

Geppert M, Goda Y, Hammer RE, Li C, Rosahl TW, Stevens CF, Sudhof TC. Synaptotagmin I: a major Ca^{2+} sensor for transmitter release at a central synapse. Cell. 1994; 79:717–727. [PubMed: 7954835]

Greengard P, Valtorta F, Czernik AJ, Benfenati F. Synaptic vesicle phosphoproteins and regulation of synaptic function. Science. 1993; 259:780–785. [PubMed: 8430330]

Hanson JE, Blank M, Valenzuela RA, Garner CC, Madison DV. The functional nature of synaptic circuitry is altered in area CA3 of the hippocampus in a mouse model of Down syndrome. J. Physiol. 2007; 579:53–67. [PubMed: 17158177]

Holtzman DM, Santucci D, Kilbridges J, et al. Developmental abnormalities and age-related neurodegeneration in a mouse model of Down syndrome. Proc. Natl. Acad. Sci. USA. 1996; 93:13,333–13,338. [PubMed: 8552589]

Hunter CL, Bimonte HA, Granholm A-CE. Behavioral comparison of 4 and 6 month-old Ts65Dn mice: Age-related impairments in working and reference memory. Behav. Brain Res. 2003; 138:121–131. [PubMed: 12527443]

Hyde LA, Crnic LS. Age-related deficits in context discrimination learning in Ts65Dn mice that model Down's syndrome and Alzheimer's disease. Behav. Neurosci. 2001; 115:1239–1246. [PubMed: 11770055]

Kleschevnikov AM, Belichenko PV, Villar AJ, Epstein CJ, Malenka RC, Mobley WC. Hippocampal long-term potentiation suppressed by increased inhibition in the Ts65Dn mouse, a genetic model of Down syndrome. J. Neurosci. 2004; 24:8153–8160. [PubMed: 15371516]

Kurt MA, Davies DC, Kidd M, Dierssen M, Florez J. Synaptic deficit in the temporal cortex of partial trisomy 16 Ts65Dn mice. Brain Res. 2000; 858:191–197. [PubMed: 10700614]

Lejeune J, Turpin R, Gautier M. Le mongolisme, premier exemple d'aberration autosomique humain. Ann. Genet. 1959; 1:92–101.

Malenka RC, Bear MF. LTP and LTD: an embarrassment of riches. Neuron. 2004; 44:5–21. [PubMed: 15450156]

Malinow R, Malenka RC. AMPA receptor trafficking and synaptic plasticity. Annu. Rev. Neurosci. 2002; 25:103–126. [PubMed: 12052905]

Marin-Padilla M. Structural abnormalities of the cerebral cortex in human chromosomal aberrations: a Golgi study. Brain Res. 1972; 44:625–629. [PubMed: 4263073]

Marin-Padilla M. Pyramidal cell abnormalities in the motor cortex of a child with Down's syndrome. A Golgi study. J. Comp. Neurol. 1976; 167:63–81. [PubMed: 131810]

Nadel L. Down's syndrome: a genetic disorder in biobehavioral perspective. Genes Brain Behav. 2003; 2:156–166. [PubMed: 12931789]

Olson LE, Roper RJ, Baxter LL, Carlson EJ, Epstein CJ, Reeves RH. Down syndrome mouse models Ts65Dn, Ts1Cje, and Ms1Cje/Ts65Dn exhibit variable severity of cerebellar phenotypes. Dev. Dyn. 2004; 230:581–589. [PubMed: 15188443]

Patel MR, Lehrman EK, Poon VY, Crump JG, Zhen M, Bargmann CI, Shen K. Hierarchical assembly of presynaptic components in defined C. elegans synapses. Nat Neurosci. 2006; 9:1488–1498. [PubMed: 17115039]

Pollonini G, Gao V, Rabe A, Palminiello S, Albertini G, Alberini CM. Abnormal expression of synaptic proteins and neurotrophin-3 in the Down syndrome mouse model Ts65Dn. Neuroscience. 2008; 156:99–106. [PubMed: 18703118]

Reeves RH, Irving NG, Moran TH, et al. A mouse model for down syndrome exhibits learning and behavior deficits. Nat. Genet. 1995; 11:177–184. [PubMed: 7550346]

Richtsmeier JT, Baxter LL, Reeves RH. Parallels of craniofacial maldevelopment in Down syndrome and Ts65Dn mice. Dev. Dyn. 2000; 217:137–145. [PubMed: 10706138]

Richtsmeier JT, Zumwalt A, Carlson EJ, Epstein CJ, Reeves RH. Craniofacial phenotypes in segmentally trisomic mouse models for Down syndrome. Am. J. Med. Genet. 2002; 107:317–324. [PubMed: 11840489]

Schmidt-Sidor B, Wisniewski K, Shepard T, Sersen E. Brain growth in Down syndrome subjects 15-22 weeks of gestational age at birth to 60 months. Clin. Neuropathol. 1990; 9:181–190. [PubMed: 2146054]

Schoch S, Gundelfinger ED. Molecular organization of the presynaptic active zone. Cell Tissue Res. 2006; 326:379–391. [PubMed: 16865347]

Shen K, Teruel MN, Connor JH, Shenolikar S, Meyer T. Molecular memory by reversible translocation of calcium/calmodulin-dependent protein kinase II. Nat. Neurosci. 2000; 3:881–886. [PubMed: 10966618]

Sheng M, Hoogenraad CC. The postsynaptic architecture of excitatory synapses: a more quantitative view. Annu. Rev. Biochem. 2007; 76:823–847. [PubMed: 17243894]

Siarey RJ, Stoll J, Rapoport SI, Galdzicki Z. Altered long-term potentiation in the young and old Ts65Dn mouse, a model for Down syndrome. Neuropharmacology. 1997; 36:1549–1554. [PubMed: 9517425]

Siarey RJ, Carlson EJ, Epstein CJ, Balbo A, Rapoport SI, Galdzicki Z. Increased synaptic depression in the Ts65Dn mouse, a model for mental retardation in Down syndrome. Neuropharmacology. 1999; 38:1917–1920. [PubMed: 10608287]

Siarey RJ, Kline-Burgess A, Cho M, Balbo A, Best TK, Harashima C, Klann E, Galdzicki Z. Altered signaling pathways underlying abnormal hippocampal synaptic plasticity in the Ts65Dn mouse model of Down syndrome. J. Neurochem. 2006; 98:1266–1277. [PubMed: 16895585]

Siddiqui A, Lacroix T, Stasko MR, Scott-McKean JJ, Costa ACS, Gardiner KJ. Molecular responses of the Ts65Dn and Ts1Cje mouse models of Down syndrome to MK-801. Genes Brain Behav. 2008; 7:810–820. [PubMed: 19125866]

Sudhof TC, Lottspeich F, Greengard P, Mehl E, Jahn R. A synaptic vesicle protein with a novel cytoplasmic domain and four transmembrane regions. Science. 1987; 238:1142–1144. [PubMed: 3120313]

Sudhof TC. Neuroligins and neurexins link synaptic function to cognitive disease. Nature. 2008; 455:903–911. [PubMed: 18923512]

Suetsugu M, Mehraein P. Spine distribution along the apical dendrites of the pyramidal neurons in Down's syndrome. A quantitative Golgi study. Acta Neuropathol. 1980; 50:207–210. [PubMed: 6447982]

Takashima S, Becker LE, Armstrong DL, Chan F-W. Abnormal neuronal development in the visual cortex of the human fetus and infant with Down's syndrome. A quantitative and qualitative Golgi study. Brain Res. 1981; 225:1–21. [PubMed: 6457667]

Trinidad JC, Specht CG, Thalhammer A, Schoepfer R, Burlingame AL. Comprehensive identification of phosphorylation sites in postsynaptic density preparations. Mol. Cell. Proteomics. 2006; 5:914–922. [PubMed: 16452087]

Trinidad JC, Thalhammer A, Specht CG, Lynn AJ, Baker PR, Schoepfer R, Burlingame AL. Quantitative analysis of synaptic phosphorylation and protein expression. Mol. Cell. Proteomics. 2008; 7:684–696. [PubMed: 18056256]

Turrigiano GG, Leslie KR, Desai NS, Rutherford LC, Nelson SB. Activity-dependent scaling of quantal amplitude in neocortical neurons. Nature. 1998; 391:892–896. [PubMed: 9495341]

Turrigiano GG, Nelson SB. Hebb and homeostasis in neuronal plasticity. Curr. Opin. Neurobiol. 2000; 10:358–364. [PubMed: 10851171]

Wagh DA, Rasse TM, Asan E, Hofbauer A, Schwenkert I, Durrbeck H, Buchner S, Dabauvalle MC, Schmidt M, Qin G, Wichmann C, Kittel R, Sigrist SJ, Buchner E. Bruchpilot, a Protein with Homology to ELKS/CAST, Is Required for Structural Integrity and Function of Synaptic Active Zones in Drosophila. Neuron. 2006; 49:833–844. [PubMed: 16543132]

Waites CL, Craig AM, Garner CC. Mechanisms of vertebrate synaptogenesis. Annu. Rev. Neurosci. 2005; 28:251–274. [PubMed: 16022596]

Walikonis RS, Jensen ON, Mann M, Provance DW, Mercer JA, Kennedy MB. Identification of proteins in the postsynaptic density fraction by mass spectrometry. J. Neurosci. 2000; 20:4069–4080. [PubMed: 10818142]

Wenger GR, Schmidt C, Davisson MT. Operant conditioning in the Ts65Dn mouse: Learning. Behav. Genet. 2004; 34:105–119. [PubMed: 14739701]

Willemsen R, Oostra BA, Bassell GJ, Dictenberg J. The fragile X syndrome: from molecular genetics to neurobiology. Ment Retard Dev Disabil Res Rev. 2004; 10:60–67. [PubMed: 14994290]

Ziv NE, Garner CC. Cellular and molecular mechanims of presynaptic assembly. Nat. Rev. Neurosci. 5:385–399. [PubMed: 15100721]

Zoghbi HY. Postnatal neurodevelopmental disorders: Meeting at the synapse? Science. 2003; 302:826–830. [PubMed: 14593168]

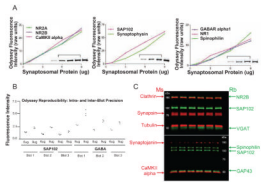

Figure 1. Western blot analysis with the Odyssey imaging system

(A) All antibodies used to quantify proteins in WT and Ts65Dn synaptosomes were calibrated to determine the linear range of detection. Representative signal plots show that this range was generally between 3–9 μg of synaptosomal material. (A, *inserts*) Western blotting (1, 3, 6, 9, and 11-μg sample loaded sequentially left to right) for CamKIIα, SAP102 and $GABA_A$α1. Overhanging brackets indicate the 3–9 μg lanes. (B) The Odyssey system can reliably detect defined amounts of protein within and between blots. Probing for SAP102 and $GABA_A$α1 generates comparable fluorescence intensities. (C) The Odyssey system in practice. With the use of differentially labeled secondary antibodies, multiple synaptic proteins can be surveyed at once with virtually no signal overlap (WT, Ts65Dn triplicates are shown left to right). Ms (red), mouse; Rb (green), rabbit.

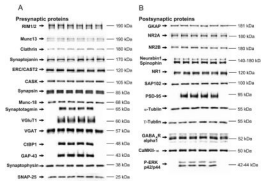

Figure 2. Protein conservation in Ts65Dn synaptosomes

(A,B) Probing for key presynaptic and postsynaptic proteins shows few differences between the makeup of WT and Ts65Dn synaptosomes beyond the expression of synaptojanin, a protein upregulated in Ts65Dn (WT, Ts65Dn duplicates or triplicates are displayed left to right; 6 μg per lane).

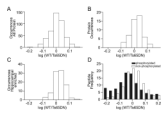

Figure 3. Overall comparison between WT and Ts65Dn synapses

(A) Everything considered, protein levels did not display a large degree of variation between WT and Ts65Dn mice. A histogram from two biological replicates of synapses shows that the $\log_{10}$ average protein expression had a very small spread. 442 proteins were quantified using three or more unique peptides, and approximately 95% of the expression ratios were within +/− 0.108 $\log_{10}$ units (corresponding to a range of 0.78 to 1.28 for the WT/Ts65DN ratios). (B) For the same set of experiments, we examined the distribution for the subset of proteins annotated as “synaptic” in the Gene Ontology database (a total of 52 proteins). (C) We also examined the distribution for a subset of proteins found to be enriched in the hippocampus (a total of 96) in a previous study (Trinidad *et al.* 2008). For both of these subsets, the distributions were approximately as narrow as that for the entire dataset. Figure 3(D) shows the distribution of phosphopeptides for proteins identified with three or more unique peptides (*black bars*, 641 phosphopeptides). The phosphorylation ratios showed a higher degree of spread. Only 70% of the phosphopeptides had expression ratios within +/− 0.108 $\log_{10}$ units. Because peptide-level measurements should exhibit a larger variance than protein-level measurements (composed of averages of many peptides), we also plotted the expression ratios of non-phosphoryalted peptides from proteins found to be phosphorylated (*white bars*, 2178 peptides). Phosphopeptides displayed a clear shift towards lower WT/Ts65DN ratios, consistent with an average increase in phosphorylation stoichiometry in the Ts65Dn mouse of approximately 7%.

Table 1

Odyssey Fluorescence Values

Summary of fluorescence values obtained for proteins examined in WT and Ts65Dn synaptosomes via Western blot and Odyssey visualization. All WT and Ts65Dn samples were loaded in duplicate or triplicate in 7.5% homemade PAGE gels. For quantification purposes, the mean raw intensity value for the WT bands of a given protein in a gel-blot were divided by the mean raw intensity value for the Ts65Dn bands, creating a WT/Ts65Dn ratio for each protein. The averages of these ratios across individual blots are presented along with their standard deviations (mean ± SD). *n* indicates the number of times for which a protein was probed/blotted. WT/Ts65Dn protein ratios were evaluated via two-tailed, one-sample *t*-tests against an expected, hypothetical value of 1.0 (a value signifying no change between the WT and Ts65Dn conditions) using GraphPad Software. *P* values < 0.05 were considered significant (*).

	WT/Ts65Dn Ratio
Rim1/2	1.10 ± 0.182, *n* = 9
Munc-13	1.04 ± 0.155, *n* = 4
Clathrin	0.98 ± 0.179, *n* = 14
*Synaptojanin	0.57 ± 0.160, *n* = 6
*Erc/CAST2	1.15 ± 0.064, *n* = 10
CASK	0.96 ± 0.037, *n* = 3
Synapsin I	1.04 ± 0.092, *n* = 12
Munc-18	1.09 ± 0.157, *n* = 10
Synaptotagmin	1.09 ± 0.165, *n* = 7
VGluT1	0.97 ± 0.057, *n* = 2
VGAT	1.00 ± 0.138, *n* = 11
CtBP1	1.05 ± 0.054, *n* = 2
GAP-43	0.89 ± 0.151, *n* = 7
Synaptophysin	1.08 ± 0.140, *n* = 8
SNAP-25	1.15 ± 0.068, *n* = 2
GKAP	0.82 ± 0.117, *n* = 3
NR2A	1.11 ± 0.203, *n* = 9
NR2B	1.11 ± 0.179, *n* = 10
Spinophilin	1.01 ± 0.111, *n* = 10
NR1	1.08 ± 0.209, *n* = 12
SAP102	1.03 ± 0.116, *n* = 16
*PSD-95	1.27 ± 0.151, *n* = 12
Alpha-Tubulin	0.99 ± 0.158, *n* = 9
Tyro-Tubulin	1.03 ± 0.153, *n* = 3
*$GABA_A$ alpha 1	1.16 ± 0.134, *n* = 9
*CaMKII alpha	1.22 ± 0.194, *n* = 16
Phospho-ERK	0.86 ± 0.259, *n* = 5

Table 2

This table lists the subset of proteins showing the largest consistent increase or decrease in WT/Ts65Dn (DS) expression ratios. The columns list the Uniprot Accession numbers; Protein Names; the number of peptides identified/quantified for that entry; the WT/Ts65Dn (DS) ratio for the first biological replicate; the WT/Ts65Dn (DS) ratio for the second biological replicate; and the average of the two ratios. To be included on this table, proteins needed to be quantified using three or more unique peptides. For both sets of independent biological isolates, the proteins further needed to show an increase or decrease of 15%.

Uniprot Accession	Protein Name	Peptides	WT/DS 1	WT/DS 2	average
Q3UHG2	Unc-13 homolog A (C. elegans)	12	1.27	1.44	1.35
Q61584	Fragile X mental retardation gene 1, autosomal homolog	3	1.34	1.26	1.30
A2A4K6	Contactin associated protein-like 1	3	1.39	1.20	1.29
Q3U6C7	Succinate-Coenzyme A ligase, ADP-forming, beta subunit	3	1.32	1.24	1.28
Q3V028	Cylindromatosis (turban tumor syndrome)	5	1.26	1.28	1.27
P59281	DNA segment, Chr 15, Wayne State University 169	3	1.30	1.22	1.26
Q2UZW7	Microtubule-associated protein, RP/EB family, member 3	3	1.31	1.21	1.26
A2ARR0	Calcium channel, voltage-dependent, beta 4 subunit	4	1.23	1.24	1.23
P14206	Ribosomal protein SA	3	1.24	1.19	1.22
P60469	Liprin alpha 3	9	1.23	1.17	1.20
Q4KMR9	Similar to SEC61 gamma	8	1.24	1.16	1.20
Q6ZQ54	Neurofascin	15	0.86	0.86	0.86
A2ARN9	Microtubule-associated protein 1 A	28	0.84	0.85	0.85
Q99P72	Reticulon 4	5	0.80	0.81	0.81
Q3U5Y9	NADH dehydrogenase (ubiquinone) Fe-S protein 2	5	0.75	0.86	0.81
Q8BTZ3	NADH dehydrogenase (ubiquinone) Fe-S protein 3	4	0.85	0.75	0.80
Q60996	protein phosphatase 2A56 kDa regulatory subunit gamma	3	0.72	0.85	0.79
Q3TIT9	Acetyl-Coenzyme A acyltransferase 2	5	0.80	0.76	0.78
P17182	Enolase 1, alpha non-neuron	3	0.69	0.83	0.76
Q6ZWS6	Synaptic nuclear envelope 1	3	0.64	0.84	0.74
Q3UD06	ATP synthase gamma chain	3	0.79	0.67	0.73
P10126	Eukaryotic translation elongation factor 1 alpha 1	3	0.54	0.77	0.65
Q5SVV1	Ubiquinol-cytochrome c reductase, Rieske	4	0.78	0.51	0.64

Table 3

This table lists the subset of phosphopeptides showing the largest consistent increase or decrease in WT/Ts65Dn (DS) ratios. The columns list the Protein Names; the sequence of the phosphopeptide; the number of peptides identified/quantified for that entry; the WT/Ts65Dn (DS) ratio for the first biological replicate; the WT/Ts65Dn (DS) ratio for the second biological replicate; and the average of the two ratios. For the peptide sequence, lower case "*s*, *t*, or *y*" designates the site of phosphoryaltion. If multiple sites are enclosed in parenthesis, the exact site of phosphorylation could not be determined from the MS/MS spectra. Lower case "*m*" refers to oxidation of methionine. To be included on this table, phosphopeptides needed to be quantified from proteins identified by at least three unique peptides. For both sets of independent biological isolates, the peptides further needed to show an increase or decrease of 15%.

Protein Name	Peptide	WT/DS 1	WT/DS 2	average
Discs, large homolog 4 (PSD-95, SAP-90)	EQLmN(ssLGsGtAsLRs)NPK	4.14	1.21	2.67
CaMKII α/γ/δ	AGAYDFPsPEWDTVTPEAK	3.45	1.62	2.54
Armadillo repeat deleted in velo-cardio-facial syndrome	sLAADDEGGPDLEPDYSTATR	1.62	2.40	2.01
Glutamate receptor, ionotropic, NMDA2A (epsilon 1)	YLPEEVAH(sDIs)ETSSR	2.29	1.50	1.89
Glutamate receptor, ionotropic, NMDA2B (epsilon 2)	NmANLSGVNGsPQSALDFIRR	2.00	1.73	1.87
Piccolo (presynaptic cytomatrix protein)	TTLYFDEEPELEmESL(tDs)PEDR	1.35	1.84	1.60
Centaurin, gamma 1	LK(sFGs)LR	1.43	1.63	1.53
Liprin alpha 3	SLPGsALELR	1.37	1.68	1.52
Discs, large homolog-associated protein 1	SLDSLDPAGLLTsPK	1.72	1.31	1.51
Liprin alpha 3	RGsALGPDEAGGELER	1.76	1.25	1.50
Dynein cytoplasmic 1 light intermediate chain 1	DFQEYVEPGEDFPAsPQR	0.57	0.40	0.48
RIKEN cDNA 2010300C02 gene	DTSLPKGD(tPPPEtItDt)NLETPSDTER	0.37	0.60	0.48
Signal-induced proliferation-associated 1 like 1	FLmPEAYP(ss)PR	0.37	0.55	0.46
Leucine rich repeat containing 7	GGLEGQS(sls)mTDPQFLK	0.38	0.53	0.46
Erythrocyte protein band 4.1-like 3	GI(sQt)NLITTVTPEK	0.34	0.52	0.43
Reticulon 4	Acetyl-mEDIDQSSLVSSSADsPPRPPPAFK	0.59	0.27	0.43
Dynamin 1	SGQAsPSRPESPRPPFDL	0.31	0.54	0.43
Piccolo (presynaptic cytomatrix protein)	LPSP(tsPLs)PHSNK	0.40	0.33	0.36
Adducin 2 (beta)	SPS(tEs)QLmSK	0.42	0.27	0.35
Synapsin I	LP(sPt)AAPQQSASQATPVTQGQGR	0.10	0.29	0.20

Table 4

A brief summary of the Ts65Dn synaptic proteomics literature.

Authors	Tissue	Proteins surveyed	Results
Siarey et al., 2006	Whole Hippocampus	CaMKIIα, pCaMKIIα, Akt, pAkt, ERK1/2, pERK1/2, GluR1, pSer831-GluR1, pSer845-GluR1	↑ pCaMKIIα, pAkt, GluR1, pSer831-GluR1 ↓ pERK1/2
	Hippocampal Synaptosomes	GluR1, pSer831-GluR1	↓ pSer831-GluR1
Pollonini et al., 2008	Whole Hippocampus	Synaptophysin, Synapsin, MAP2, PSD-95, Spinophilin, Gephyrin, CDK5, pCREB, C/EBPβ, MuSK, NR1, GluR1, GluR2, GluR3	↓ Synaptophysin ↑ CDK5
Siddiqui et al., 2008	Cortex, Soluble and Crude Membrane Fractions	TIAM1, Dyrk1A, ITSN1, Akt, pAkt (Ser473), ERK1/2, pERK1/2(Tyr204) NR1, pNR1 (Ser897), pELK, pGSK3B	↑ TIAM1, Dyrk1A (membrane) ↑ ITSN1, pAkt, pGSK3B (soluble)
	Hippocampus, Soluble and Crude Membrane Fractions	TIAM1, Dyrk1A, ITSN1, Akt, pAkt, ERK1/2, pERK1/2, NR1, pNR1, pELK	↑ TIAM1, Dyrk1A, ITSN1, pAkt, pERK1/2, pELK (soluble)
Belichenko et al., 2009	Whole Hippocampus	$GABA_A\alpha1$, $GABA_A\beta2$, $GABA_A\beta3$, $GABA_BR1$, $GABA_BR2$, Neuroligin 1 & 2, GluR1,GluR2	↔ No changes